Plasminogen activator-coated nanobubbles targeting cell-bound β2-glycoprotein I as a novel thrombus-specific thrombolytic strategy

Paolo Macor,[1] Paolo Durigutto,[2] Monica Argenziano,[3] Kate Smith-Jackson,[4] Sara Capolla,[5] Valeria Di Leonardo,[1] Kevin Marchbank,[4] Valerio Stefano Tolva,[6] Fabrizio Semeraro,[7] Concetta T. Ammollo,[7] Mario Colucci,[7] Roberta Cavalli,[3] Pierluigi Meroni[2] and Francesco Tedesco[2]

[1]Department of Life Sciences, University of Trieste, Trieste, Italy; [2]Istituto Auxologico Italiano, IRCCS, Laboratory of Immuno-Rheumatology, Milan, Italy; [3]Department of Scienza e Tecnologia del Farmaco, University of Turin, Turin, Italy; [4]Translational and Clinical Research Institute, Faculty of Medical Sciences, Newcastle University, Newcastle, UK; [5]Experimental and Clinical Pharmacology Unit, C.R.O.-IRCCS, Aviano, Italy; [6]Struttura Complessa di Chirurgia Vascolare, ASST GOM Niguarda. Milano, Italy and [7]Dipartimento di Scienze Biomediche e Oncologia Umana, Università degli Studi di Bari Aldo Moro, Bari, Italy

Correspondence: P. Macor
pmacor@units.it

Received: June 8, 2022.
Accepted: September 22, 2022.
Early view: September 29, 2022.

https://doi.org/10.3324/haematol.2022.281505

SUPPLEMENTARY APPENDIX

Plasminogen activator-coated nanobubbles targeting cell-bound β2-glicoprotein I as a novel thrombus-specific thrombolytic strategy

Paolo Macor[1*], Paolo Durigutto[2], Monica Argenziano[3], Kate Smith-Jackson[4], Sara Capolla[5], Valeria Di Leonardo[1], Kevin Marchbank[4], Valerio Stefano Tolva[6], Fabrizio Semeraro[7], Concetta T. Ammollo[7], Mario Colucci[7], Roberta Cavalli[3], Pierluigi Meroni[2], Francesco Tedesco[2]

[1]Department of Life Sciences, University of Trieste, 34127 Trieste, Italy; [2]Istituto Auxologico Italiano, IRCCS, Laboratory of Immuno-Rheumatology, Milan, Italy; [3]Department of Scienza e Tecnologia del Farmaco, University of Turin, 10125 Turin, Italy; [4]Translational and Clinical Research Institute, Faculty of Medical Sciences, Newcastle University, Newcastle, UK; [5]Experimental and Clinical Pharmacology Unit, C.R.O.-IRCCS, 33081 Aviano, Italy; [6]Struttura Complessa di Chirurgia Vascolare, ASST GOM Niguarda. Milano, Italy; [7]Dipartimento di Scienze Biomediche e Oncologia Umana, Università degli Studi di Bari Aldo Moro, Bari, Italy.

Supplementary Methods

Nanobubbles preparation and characterization

Targeted NBs were prepared by chemical conjugation of MBB2DCH2, a CH2-deleted variant of scFv-Hinge-CH2-CH3 recombinant antibody directed against the DI domain of β2-GPI. [11] The recombinant antibody was oxidized by periodate oxidation and conjugated by reductive amination to chitosan amino groups. NBs were then loaded with rtPA from Boehringer Ingelheim (Milan, Italy; 1mg/ml) to the final concentration of 100 μg/ml NB suspension through covalent conjugation of the thrombolytic agent either by amino-reductive reaction (Type A) or by carbodiimide-mediated amide bond formation (Type B). The amount of rtPA loaded on NBs was measured by the Pierce™ BCA protein assay kit (Thermo Scientific, Rockford, IL USA). One ml of the BCA reagent was added to 100 μl of the sample and reacted for 30 min at 37 °C. After cooling to room temperature, the chromogenic product was measured by an UV-Vis spectrophotometer at 562 nm. The rtPA concentration was calculated with reference to a calibration curve constructed with rtPA standard solutions in the concentration range between 0 - 200 μg/ml. Fluorescent NBs formulations were prepared by labeling the NB core with coumarin 6. The encapsulation efficiency and loading capacity of the rtPA-loaded NBs were calculated using the following equations: Encapsulation efficiency = [amount of rtPA loaded/total amount of rtPA] x 100 and Loading capacity = [amount of rtPA loaded/total weight of NBs] x 100. NB formulations were characterized determining their physico-chemical properties. The size, polydispersity index and surface charge were determined by dynamic light scattering technique (DLS) using a 90 Plus instrument (Brookhaven, NY, USA). The analyses on diluted NB samples (1:30 v/v in filtered water) were performed at a scattering angle of 90°C and a temperature of 25°C. Nanobubble morphology was investigated by transmission electron microscopy (TEM) using a High Resolution JEOL 300 kV microscope. The diluted NBs were stained with osmium tetroxide aqueous solution (0.1% v/v) before TEM analysis. After dropping the sample on the copper grid, it was blotted onto a filter paper and air dried before analysis. The physical stability of NB formulations stored at 4° C was investigated up to 6 months, evaluating the physico-chemical parameters and the rtPA content and activity of NBs over time.

Immunofluorescence analysis

Seven μm sections of patients' thrombi or in vitro blood clots were stained with the following antibodies (5μg/ml): FITC-labeled mouse anti-human CD9 (ImmunoTools, Friesoythe, Germany); rabbit anti-human β2-GPI (Sigma, Milan, Italy) revealed by CY3-labeled sheep anti-rabbit IgG

(Sigma). The slides were mounted with the Mowiol-based antifading medium (Sigma) and the images were acquired with the fluorescence microscope Leica DM2000 equipped with Leica DFC420 camera.

For studies in C3 gain-of-function (GOF) mice, 5µm cryosections from mouse kidneys were mounted on a Shandon ColorFrost Plus microscope slide (Thermo Scientific), and stored at -80°C. To detect fibrin, thawed tissue sections were fixed in acetone, blocked for 30 minutes in rabbit serum and then incubated with sheep anti-human fibrinogen (Bio-Rad, Milan, Italy) for 1 hour, followed by rabbit anti-sheep IgG Alexa 555 (Abcam, Cambridge, UK). After incubation with the secondary antibodies, the slides underwent repeated washing with PBS, then stained with DAPI, covered with glass coverslip and fluorescence images were taken at x20 on Leica DM2000 LED using a Leica DFC 7000 T camera. Densitometry analysis of Glomerular Fibrin deposition was performed using FiJi (Image J, NIH).

In vitro fibrinolytic and thrombolytic assays

The experiments to investigate the functionality of rtPA-coated NBs were carried out in microplate wells. NBs loaded with rtPA (5 µl) or soluble rtPA (5 µl) were added to human plasma (50 µl) and clot formation was induced by 10 µl thromboplastin (Recombiplastin, Wefen, Milan, 1:1000 final dilution) and 50 µl $CaCl_2$ (20 mM). The rate of lysis (1/lysis time) was calculated by the changes in optical density measured at 405 nm.

The thrombolytic activity of targeted and untargeted rtPA-NBs was evaluated in models consisting of FITC-labeled platelet-rich human blood clots (Chandler thrombi, ~100 µl) submerged in autologous plasma (0.49 ml). In these experiments NBs or rtPA (10 µl) were added to the bathing plasma, thereby mimicking the thrombolytic process. The percent of lysis was determined at fixed intervals by measuring the release of FITC-labeled fibrin degradation products.

APS model

The APS model was established in rats that were intraperitoneally injected with LPS (2.5 mg/kg) and then anesthetized with Zoletil (Virbac, 25 mg/Kg) and Xylazine (Rompun, 7,5mg/kg). Afterwards, they received a slow infusion of Rhodamine 6G (Sigma) into the jugular vein, to stain leukocytes and platelets, followed by infusion of 1 ml of pooled sera from 5 APS patients containing antibodies to β2-GPI into the carotid artery to cause thrombus formation, which occurred in a time range of 15-25 min. Targeted and untargeted NBs (30 µg of bound rtPA in 300 µl saline; ~ 0,1 µg/g body weight) or free rtPA (300 µg of rtPA in 300 µl saline; ~ 1 µg/g body weight) were then infused

into the carotid artery and the formation of thrombi in the mesenteric vessels was monitored by intravital microscopy. The percentage of occluded vessels was evaluated by measuring the blood flow.

Ferric chloride induced thrombosis

Thrombosis was induced in anesthetized rats following an incision made through the abdominal wall to exteriorize the ileal mesentery. After careful analysis to ascertain the integrity of mesenteric vasculature, bands of filter paper soaked with 0.6% ferric chloride ($FeCl_3$) were placed on the ileal mesentery for 3 minutes. Eight to 10 minutes after removal of the filter paper, generated thrombi were visualized by intravital staining with Rhodamine 6G. Targeted and untargeted NBs (60 µg of bound rtPA in 300 µl saline; ~ 0,2 µg/g body weight) or free rtPA (600 µg of rtPA in 300 µl of saline; ~ 2 µg/g body weight) were injected soon after thrombus formation. The percentage of occluded vessels was evaluated by measuring the blood flow.

C3 GOF mouse model of atypical hemolytic uremic syndrome

The model of atypical hemolytic uremic syndrome (aHUS) was established in mice. In brief, a point mutation in the C activation protein C3 (C3.p. D1115N), associated with aHUS in man, was transferred to C57Bl/6J mice. The mice develop a spontaneous thrombotic microangiopathy, with microvascular fibrin deposition in the glomeruli. The phenotype can be rescued through C5 inhibition or C5 genetic knockout, thus akin to aHUS in man. Mice that developed spontaneous disease (identified by haematuria >80g/L for 48 hours) were entered into the study. Mice were randomized to receive rtPA-tNBs or rtPA-NBs (0,5µg/g body weight) or saline. The animals were dosed via the intraperitoneal route on days 0, 2 and 5 (total of 3 doses) and then culled 24 hours after the last injection. Mouse kidneys were harvested, placed in an embedding cassette, immersed in OCT and frozen on dry ice. The tissue was then stored at -80 until immunofluorescence analysis as detailed above.

Supplementary Results

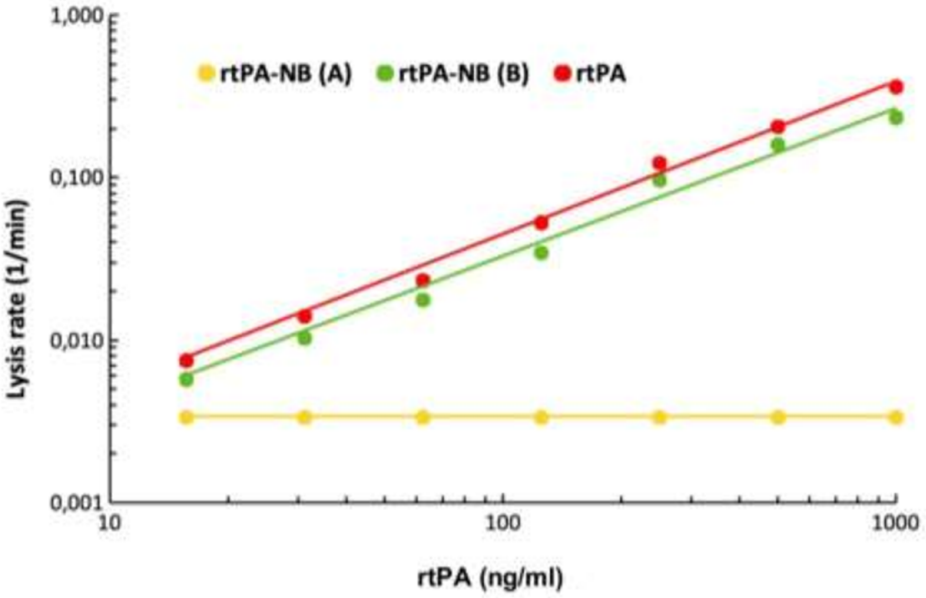

Figure S1: Fibrinolytic activity of two different types of rt-PA-coated NPs.

Increasing concentrations of either rtPA-NB (A) or rtPA-NB (B) were added to plasma, which was then clotted by thromboplastin and $CaCl_2$. Soluble rt-PA was tested in parallel for comparison. Clot lysis was monitored by the changes in optical density and expressed as lysis rate (i.e., 1/lysis time in minutes). Optical density was measured at 405 nm. The results are presented as mean of 3 independent experiments.

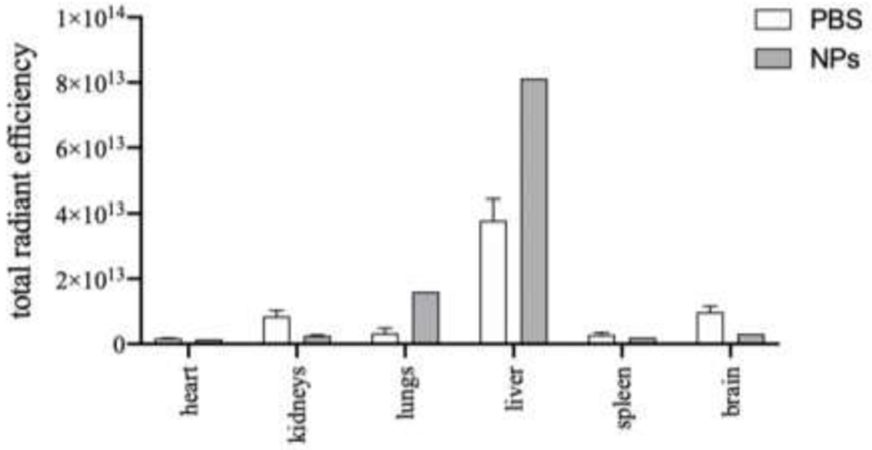

Figure S2: In vivo biodistribution of tNBs.

Cyanine 5.5-labeled tNBs were injected in LPS-stimulated rats and the near infrared fluorophore cyanine 5,5 was detected by optical imaging. The figure shows localization of the nanostructures in heart, kidneys, lungs, liver, spleen and brain as compared with organs from LPS-stimulated rats receiving either NBs or PBS and documents the typical elimination by macrophages in liver and lungs.

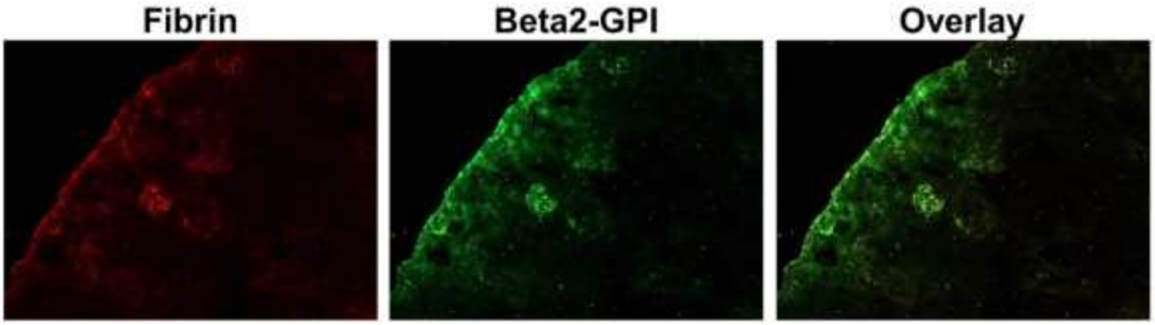

Figure S3: β2-GPI in kidneys from C3 GOF mice.

Cryosection from mouse kidney were incubated with sheep anti-human fibrinogen followed by rabbit Anti-Sheep IgG Alexa 555 to detect fibrin deposits (red) and with rabbit anti human β2-GPI revealed by sheep anti-rabbit IgG CY3 to detect β2-GPI (green). Note localization of fibrin and β2-GPI in the glomeruli and renal vessels.

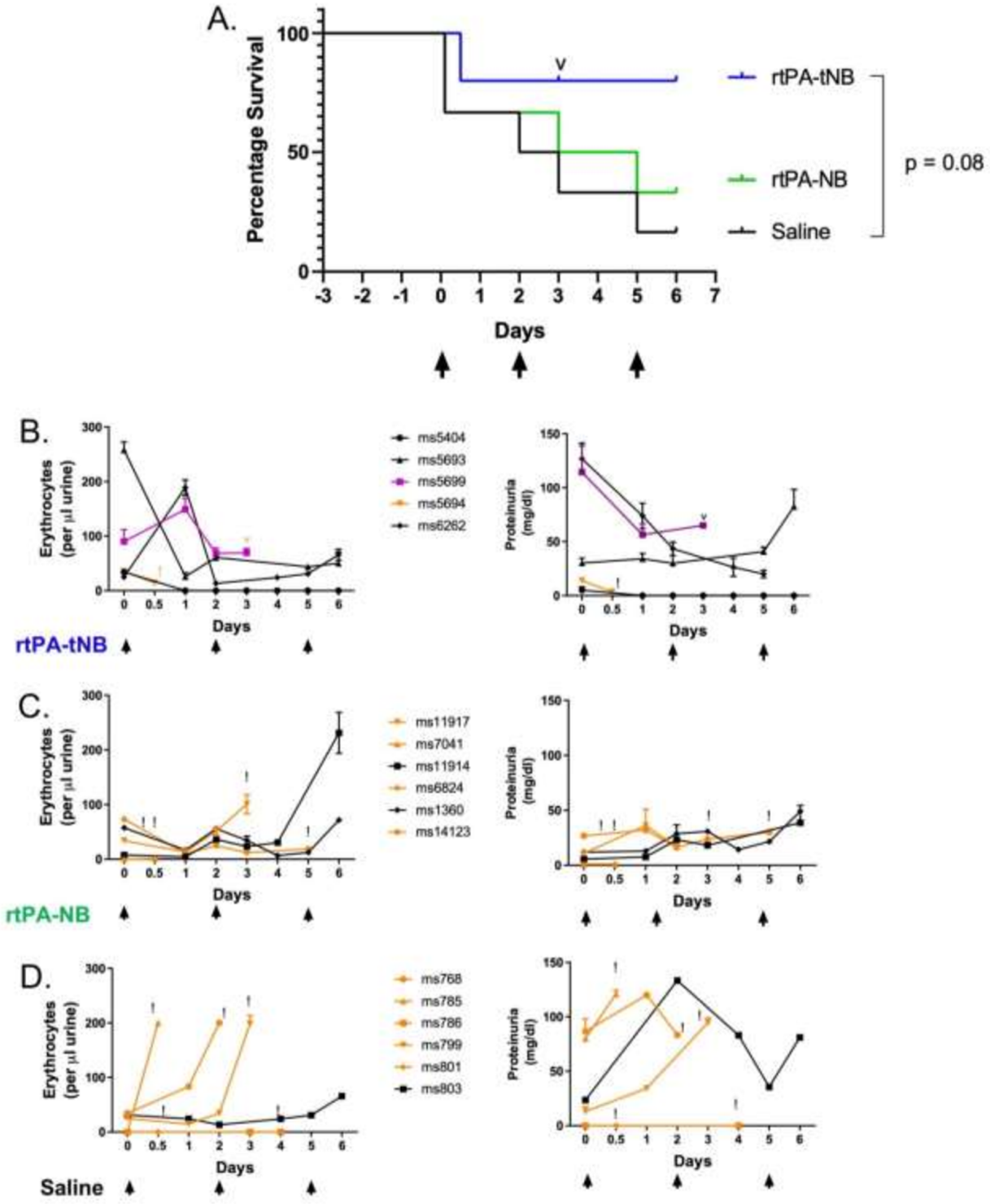

Figure S4: rtPA-tNBs dissolve clots in the C3 GOF mouse model of aHUS

A) Survival data of C3 GOF mice given saline only (n=6; Black), treated with rtPA-NB (n=7; green) or treated with rtPA-tNB (n=5; Blue). (B) Densitometry analysis using Adobe Photoshop CS3 from digital photograph of Combistix (Siemens) after 1 minute exposure to collected urine. The inverse ratio in 'eye drop' red channel (3 spatial reads) was interpolated from the reference scale (digital photograph) using 4PL. Hematuria (left panel) and proteinuria (right) of C3 GOF mice

treated with rtPA-tNB. Orange lines and ! denotes loss of mouse, treatment is indicated by arrows and substance indicated to the left. ^ and purple line denotes intervention by vet (mouse removed from study at this point). (C). hematuria (left panel) and proteinuria (right) of C3 GOF mice treated with rtPA-NB. (D). hematuria (left panel) and proteinuria (right) of C3 GOF mice given saline control. Note: When urine volume was limited, hematuria analysis was favored over proteinuria. No signal on combistix or no urine was entered as zero/blank.

Movie S1. Targeted NB accumulation in thrombi developed in a rat model of APS.

Targeted NBs labeled with coumarin 6 were injected into rat soon after the formation of thrombi induced by the administration of antibodies to β2-GPI and their in vivo distribution was followed by intravital microscopy. The NBs start localizing on thrombi already 30 seconds after injection and accumulate progressively being clearly visible after 15 min.

Movie S2. Untargeted NB accumulation in thrombi developed in a rat model of APS.

The experiment was conducted as reported in the legend to movie S1. Note that the untargeted NBs were barely detectable on intravascular thrombi.

Movie S3. Effect of rtPA-tNB on thrombus dissolution and vascular occlusion in APS model.

Targeted NBs bearing rtPA were injected into rat soon after the formation of thrombi induced by the administration of antibodies to β2-GPI and their ability to dissolve the formed thrombi was monitored with intravital microscopy. Note the rapid dissolution of the thrombi that occurred within 1 min after the injection of rtPA-tNB and persisted up to the 90-min observation

Movie S4. Effect of rtPA on thrombus dissolution and vascular occlusion in APS model.

The experiment was conducted as reported in the legend to movie S3. Note that soluble rtPA caused a less rapid dissolution of thrombi than rtPA-tNB that was nearly complete 15 min after rtPA injection, but failed to prevent formation of new thrombi clearly seen at 90 min post-injection.

Movie S5. Effect of rtPA-NB on thrombus dissolution and vascular occlusion in APS model.

The experiment was conducted as reported in the legend to movie S3. Untargeted NBs coated with rtPA failed to dissolve the thrombi that persisted throughout the experiment.

Movie S6. Effect of rtPA-tNB on vascular thrombi induced by ferric chloride.

Targeted NBs bearing rtPA were injected into rat soon after the formation of thrombi induced by the local application of ferric chloride and their thrombolytic effect was evaluated using intravital microscopy. Dissolution of thrombi started to be seen 1 min after NB administration and was definitely more marked at 15 min persisting until 90 min.

Movie S7. Effect of rtPA on vascular thrombi induced by ferric chloride.

The experiment was conducted as reported in the legend to movie S6. The thrombolysis induced by soluble rtPA started to be seen 15 min after the injection of the fibrinolytic agent and was no longer observed at 90 min.

Movie S8. Effect of rtPA-NB on vascular thrombi induced by ferric chloride.

The experiment was conducted as reported in the legend to movie S6. Note that the markedly reduced blood flow caused by thrombi remained unchanged following the administration of the untargeted NBs coated with rtPA.